Beam Halo Monitoring at CDF

Muge Karagoz Unel [a] , Richard J. Tesarek [b]

[a]*Northwestern University, Evanston, IL 60208, USA*

[b]*Fermilab, Batavia, IL 60510, USA*

Abstract

Losses from the proton and antiproton beams of the Fermilab Tevatron have been shown to produce a halo which contribute to backgrounds to physics signals in the Collider Detector at Fermilab (CDF). To provide a measure of the beam halo and losses, we have installed arrays of scintillation counters on both sides of the CDF detector. We describe here the physical configuration of these counters, their implementation and performance within the Fermilab Accelerator Control Network (ACNET). We show correlations between these new devices and the accelerator operating conditions. We point out that the use of these monitors is leading to improvement in the accelerator operations and reduced backgrounds in CDF.

Key words: Radiation detectors, radiation monitoring, beam monitors, beam halo and losses, Tevatron, CDF
PACS: 29.40.-n, 28.41.Te, 41.85.Qg

1 Introduction

The Run II program for the Tevatron started in 2001 and the CDF experiment has been taking data with recent luminosities comparable with the peak luminosity obtained at the end of Run I [1]. However, the CDF detector has encountered operational problems and observed high backgrounds which have been correlated with proton and antiproton losses from the Tevatron.

For example, high loss rates have caused high anode currents and consequent chamber trips in most muon detectors, especially in central muon upgrade and extension (CMP, CMX) chambers [2]. A number of low voltage switching power supply failures were also observed in periods of high beam loss rates associated with Tevatron injection and aborts. [1] In addition, backgrounds in the CDF detector have been associated with a halo of particles accompanying the beam. Figure 1 shows an event display of an off-axis muon producing a hard bremsstrahlung in the central calorimeter. The muon "track" is identified by the set of contiguous towers in $\eta = -\log\left(\tan\frac{\theta}{2}\right)$ at constant azimuth (ϕ). The vertical scale is the energy in the calorimeter transverse to the beam. These events form backgrounds to physics signals involving photons and missing transverse energy.

CDF measures beam losses using the beam shower counters located closest to the CDF detector (BSC-1). The BSC-1 are small scintillation counters at a radius between 4–7 cm relative to the center of the beam pipe and located approximately 5 m on either side of the CDF interaction point (IP). Losses are calculated as the coincidence between the counter signal and beam particles passing the plane of the BSC-1. A detailed description of the BSC-1 and the loss calculation may be found elsewhere [3]. Because the BSC-1 are small, located near the beam line and near to the CDF IP, they are ideal for monitoring the small angle beam losses which affect various components in the tracking volume. However, these counters do a poor job of measuring the beam halo affecting the outer regions of the detector. Further, the raw BSC-1 photomultiplier tube (PMT) signals are unavailable due to the electronics requirements for the system. These PMTs have also shown strong afterpulsing [4]. Both of these issues make additional timing coincidences problematic.

We address these concerns by installing a set of counters (halo monitors) in the CDF collision hall. In this article, we describe the physical configuration of the halo monitors and their readout. These monitors detect the halo particles at a radial distance of about 50 cm around the beam line in full azimuthal coverage and at maximum available distance from the CDF detector. The monitors are capable of detecting particles at larger angles from the beam line and are complementary to the beam shower counters.

2 Setup

The CDF detector is located in the B0 section of the Tevatron at Fermilab. Two halo monitors are located in the west and east alcoves in the CDF collision

---

[1] These power supply failures were traced to a catastrophic, single event failure (single event burn out) in a radiation soft, power MOSFET used in the supplies.

hall, at positions $z = -1809$ cm and $z = 1664$ cm with respect to the IP. Both monitors consist of an array of four scintillator counters arranged in a non-overlapping rectangle surrounding the final focus, low β quadrupoles. Figures 2–4 illustrate the layout of the monitors.

The counters used for these monitors come from a set of spares originally manufactured for the KTeV muon identification and veto systems [7]. These counters are made of Bicron BC-412 scintillator [5] and have an active volume of $1.3 \times 15 \times 150$ cm^3. The scintillator is glued to a wedge shaped, lucite light guide which is in turn glued to an EMI-9954KB PMT [6]. Bicron, BC-600, optical cement is used for all glue joints. The end of the scintillator opposite the PMT was painted black to avoid signals from light reflected off the far end. The counter assemblies are then wrapped in aluminum foil and 76.2 μm thick black plastic. The wrapping materials are held in place using black vinyl tape. Figure 5 is a diagram of a single counter.

Each counter is characterized, after assembly, using three cosmic ray telescopes. The three telescopes identify cosmic rays passing through each end and the middle of the counters. Operating characteristics including the relative gain, dark rate and counter efficiency are recorded for each telescope as a function of PMT bias voltage with a discriminator threshold of 30 mV. The operating voltage for each counter is chosen to be 100 V above the "knee" of the efficiency vs PMT voltage (plateau) curve. The knee is defined to be the 90% efficiency point on the plateau curve as measured with the telescope farthest from the PMT. The light attenuation length of each counter is measured at the operating voltage.

A high voltage power supply (Power Designs model HV-1547) provides bias voltages for all the counter PMTs. The individual values are set by a Berkeley high voltage zener divider box. After installation, the ungated singles rate (dark current) for each counter is measured at the same discriminator settings and PMT bias voltages used during the counter production tests described above. Table 1 summarizes the operating parameters for these counters.

Beam halo is measured by forming a coincidence between the counter signals and a beam bunch signal as the bunch passes through the plane of the counter array on its way to the CDF IP. To mark the beam crossings, we use the 38 ns wide Bunch Crossing (CDF_BC) signal. The CDF_BC signal defines the CDF collision times with a repetition period of 396 ns. CDF_BC is derived from the 53 MHz Tevatron RF and is received from a "TRigger And Clock + Event Readout" (TRACER) module [8]. The TRACER module also distributes the timing signals which mark the first bunch in a revolution (CDF_B0) and CDF_ABORT which mark the "abort gaps" where there are no bunch crossings. All such accelerator timing signals are fanned out to TRACER modules. Figure 6 shows the relevant clock signals.

The counter PMT signals are brought up to a NIM crate in a CDF counting room where they are discriminated using a LeCroy 4413 discriminator (threshold 30 mV, width 20 ns). The discriminator width is set to allow for light propagation delays (8 ns) and slewing for the counters. The discriminated counter signals are carried to a Programmable Logic Unit (PLU) (LeCroy model 4516) to form the coincidence with the CDF_BC. The CDF_BC signal, originally of TTL-standards, is first converted to NIM standard and then its width is decreased to 20 ns by a discriminator (LeCroy model 621L). The resulting signal is time-aligned with the counter signals using a delay line. The time-alignment accounts for the beam particle time-of-flight (TOF) difference between the plane of the arrays and the interaction time. A Fan Input/Output Unit is utilized to obtain four copies of this signal for the proton monitor counters. Before making another four copies for the antiproton counters, an additional 5 ns delay is applied to account for TOF difference between the proton and the antiproton side. All CDF_BC duplicates are further passed through a NIM-ECL converter to be sent to the PLU. The eight outputs from the PLU are counted by CAMAC scalers. Figure 7 shows the logic diagram for the readout. The time alignment of the discriminated signals at the AND gate is shown in Figure 8.

The delay setting for halo coincidences is determined using a delay (coincidence) curve technique. Given a fixed counter signal propagation time, coincidence rates are measured as a function of the delay applied to the CDF_BC signal. We estimate the CDF_BC delay necessary for the coincidence by measuring the cable lengths, module propagation delays and calculating the flight delays. We then installed a delay cable approximately 40 ns shorter than this expected length and measured the coincidence rates incrementing the delay by 8 ns between measurements. The coincidence data is read out by visual scalers and rates are calculated by sampling for 10 seconds and dividing the counts by 10. Effects due to beam intensity variations in time are taken into account by simultaneously reading from a separate, ungated counter. The decrease observed in the rates read by the ungated counter at the end of the data taking is 6%. The coincidence rates from the counters are normalized to the rate measured with the ungated counter and delay curves are obtained using these normalized rates. The halo CDF_BC delay is chosen to correspond to the mid-points of the coincidence plateaus for all of the eight counters. Figure 9 shows the delay curves for all counters. The figure exhibits a collision peak as well as a halo peak. The collisions follow the halo signals at twice the particle TOF between the monitors and the IP. The difference of about 10 ns between the collisions for protons and antiprotons is due to the different z positions of the counter arrays. The ratio of proton to antiproton beam currents of approximately 10:1 is clearly reflected in the halo peaks. Figure 10 details the halo coincidence curves for each counter. The full width at half maximum of the coincidences is ~ 35 ns as expected.

The halo coincidence signals are read out through two CAMAC scalers (Fermilab "Beams Division" model 333 [9]). These scalers are a part of the Fermilab Accelerator Controls Network (ACNET). ACNET is a system to monitor and control the Fermilab accelerator complex. A graphical interface gives one access to accelerator data in real time and previous data from archives. The rates for the individual counters are calculated [2] using the expression:

$$\text{Rate} = \frac{N_{2,i} - N_{1,i}}{N_{2,0} - N_{1,0}} \times (\text{Rate of channel 0}), \tag{1}$$

where $N_{1,i}$ and $N_{2,i}$ are the two consecutive readings of scaler channel i which corresponds to an ACNET device. Channel 0 of both CAMAC scalers counts the Tevatron beam revolutions (period of 20.7 μs).

We also calculate the total rate of each counter array within ACNET. These summed rates, Proton Halo SuM (C:B0PHSM) and Antiproton Halo SuM (C:B0AHSM), are calculated as:

$$\text{Rate} = \frac{\sum (N_{2,i} - N_{1,i})}{N_{2,0} - N_{1,0}} \times (\text{Rate of channel 0}) \tag{2}$$

where the sum is over channels, i.

The halo monitor counters are also used to measure the "DC beam" (component of the beam not captured in bunches) by measuring the halo in the abort gaps of one Tevatron cycle. We follow the same logic and use the exact halo measurement setup except for two details: in addition to the bunch crossing signal from the TRACER module as described above, we carry an abort gap signal (CDF_ABORT) to the PLU and form the coincidence with the counters. In order to avoid contamination from the collision of the last bunch before the abort gap, 116 ns is removed from the leading edge of the duplicate CDF_ABORT gate. The abort gap coincidence signals correspond to eight scaler channels and their rates are calculated using formulae 1 and 2.

The rates calculated as in Equations 1 and 2 have been available on ACNET since April, 2002. The ACNET data for the proton and antiproton monitor total rates (C:B0**SM) are archived with a minimum update frequency of 1 Hz. The minimum data logging rate for individual counters is 1 minute in the CDF logger.

We verify the rate calculations by measuring the singles rates from ACNET and comparing these rates with those expected from previous measurements. We first measured the beam off coincidence rates using ACNET data and

---

[2] This calculation is implemented within the ACNET software framework.

calculated the expected values given the singles rates from Table 1 as a cross-check. For the calculation, we assumed a uniform, 35 ns resolving time for halo coincidences and approximately 2.4 μs for abort gap coincidences. Table 2 shows a comparison between the calculated and measured rates. The quoted uncertainties include only the statistical errors. The measured and calculated values are in good agreement.

The choice of discriminator widths for the counters, CDF_BC and CDF_ABORT gates imposes an upper limit on the rates these devices can effectively measure. The maximum (saturation) rate for the beam halo measurements is 1.7 MHz (maximum CDF_BC rate). The summed rates saturate at 4 times the above rate (6.8 MHz). The abort gap rates saturate at 4.6 MHz, limited by the discriminator width (20 ns), the retriggering time of the discriminator (2 ns) and duty factor of the CDF_ABORT signal after adjustment. The maximum rate of the summed signals is 18.4 MHz.

3 Performance of the Monitors

A first look at the performance of the monitors shows that they are indeed sensitive to the proton and antiproton losses. Figures 11 and 12 compare halo monitor rates with the beam losses measured at CDF. These data are taken during Tevatron store 1243. Note the clear features in the antiproton halo rates that are just visible in the antiproton loss rates (Figure 12). These features exist only in the antiproton monitors and are to be examined in more detail.

While commissioning the abort gap halo monitors, we found that the wide gate allows a significant accidental contamination from beam induced radioactivity. This is best illustrated in Figure 13 where the beam was aborted and the abort gap rates did not immediately go to their cosmic ray value. Performing a lifetime analysis of the above incident, one finds that three, short lived isotopes of potassium are responsible for the increase of the abort gap halo rate. This increased rate is removed by requiring a 2/4 majority in each abort gap halo measurement. The majority coincidence rates form two ACNET devices which are C:B0PAGC (proton) and C:B0AAGC (antiproton). The data logging and saturation characteristics of these devices are the same as the previously listed abort gap halo monitor devices.

The halo monitors have also been observed to correlate well with features in the Tevatron accelerator. Listed here, are the sensitivity to changes in the beam tune, beam vacuum, RF power, Tevatron electron lens (TEL) [10] failures and DØ Roman Pot [11] positions with respect to the beam line. Figures 14–17 illustrate these correlations. Figure 14 shows the rates for the abort gap monitors taken during store 1229. The halo in the abort gap monitors have a

clear response to the TEL operational changes. The rates show high frequency features following the lens being turned off (0.0 mA). As the TEL is turned back on, the rates increase abruptly with a subsequent decrease [12].

Figure 15 illustrates the correlation between the changes in the beam vacuum (T:F1IP1A) and proton halo (C:B0PHSM) rates during store 1207. The former variable is the vacuum ion gauge for the F11 sector of the Tevatron. The vacuum problems, identified here, were subsequently addressed. The vacuum pressure improved from values just under 2×10^{-6} Torr to well below 2×10^{-8} Torr yielding about 30–40% halo reduction in CDF Collision Hall.

The monitors are also capable of detecting changes along the beam lines. Figure 16 shows an abrupt increase in the antiproton halo monitor rates (C:B0AHSM) as a response to the DØ Roman Pot insertion during store 1229. The DØ detector is located at the DØ section of Tevatron, upstream of CDF in the antiproton direction. As of the writing of this article, we anticipate a controlled test with the pots to be performed.

The abort gap halo rates correlate well with sudden losses within the RF structure in Tevatron. In such cases, more particles escape from the bunches and fill the abort gaps. Figure 17 includes that portion of Tevatron store 1750 at which the power to an RF cavity is lost. Typically, the rates also continuously rise near the end of a store due to time dependent detoriation of the beam tune. This is reflected in the abort gap halo monitor (C:B0PAGC) rates.

The halo monitors are in the regular monitoring list of the CDF experiment as the halo has an impact on silicon and muon detectors. Alarms are currently notifying experimenters on shift when beam conditions move out of tolerances.

4   Conclusion

We installed two counter arrays in the CDF collision hall to improve the monitoring of beam quality. These counters are set up to monitor Tevatron halo and beam in the abort gaps with the proper choice of signal coincidences. The coincidences behave as expected under controlled conditions and new variables are installed in the Fermilab accelerator controls network (ACNET). Such monitors did not exist for Tevatron experiments during Run I. Data from these devices are shown to reproduce losses qualitatively and the devices are observed to be sensitive to effects not previously seen by existing monitors. The data also show that some beam effects are visible with an enhanced sensitivity when compared with existing detectors. The monitors are being used by the Fermilab accelerator experts in order to investigate the properties of the Tevatron beam halo as measured in the CDF collision hall. We

believe these type of monitors also serve as examples for the next generation of hadron colliders for which the background and radiation conditions will be more severe.

Acknowledgements

References

[1]   The CDF Collaboration, FERMILAB-PUB-96/390-E (1996) and references therein.

[2]   T. Dorigo, Nucl. Instr. and Meth. A **461** (2001) 560.

[3]   M. Gallinaro, FERMILAB-CONF-02-121-E (2002) 11.

[4]   M.Binkley, Particle Physics Division - CDF Department, Fermilab and R.Vidal, Particle Physics Division - CDF Department, Fermilab, private communication.

[5]   Bicron Photonics Division,
      Saint Gobain Crystals & Detectors,
      12345 Kinsman Road,
      Newbury, Ohio 44065, USA.

[6]   Electron Tubes Inc. (formerly Thorn-EMI),
      100 Forge Way, Unit F
      Rockaway, NJ 07866, USA.

[7]   A. Alavi-Harati, *et al.*, Phys. Rev. Lett. **87** (2001) 071801.

[8]   T.M. Shaw, *et al.*, IEEE Trans. Nucl. Sci. **47** (2000) 1506.

[9]   R.J. Ducar, *http://www-bd.fnal.gov/controls/camac_modules/c333.htm* (1992).

[10] V. Shiltsev, *et al.*, Phys. Rev. ST **7** (1999) 071001.

[11] A. Brandt, *et al.*, FERMILAB-PUB-97-377 (1997) 85.

[12] R.Vidal, Particle Physics Division - CDF Department, Fermilab, private communication.

Table 1

Operating parameters for scintillator counters used in the CDF collision hall alcoves.

Counter ID	PMT Bias Voltage (V)	Attenuation Length (cm)	Ungated Dark Count Rate (Hz)
083	1875	294 ± 31	50
059	1637	241 ± 41	91
042	1888	238 ± 20	32
003	1785	255 ± 23	184
054	1668	282 ± 28	114
066	1495	229 ± 18	84
014	1843	260 ± 24	22
040	1786	255 ± 22	60

Table 2

Measured and calculated beam-off rates for the halo and abort gap monitors.

| Counter | | Halo Rate (Hz) | | Abort Gap Rate (Hz) | |
ID	Device	Meas.	Calc.	Meas.	Calc.
083	B0A*N	4±2	3±2	22±5	17± 4
059	B0A*T	5±2	5±2	36±6	32± 6
042	B0A*S	2±1	2±1	14±4	11± 3
003	B0A*B	11±3	11±3	78±9	64± 8
054	B0P*N	6± 2	7± 3	45±7	40± 6
066	B0P*T	5± 2	5± 2	43±7	30± 5
014	B0P*S	1± 1	1±1	8± 3	8± 3
040	B0P*B	3± 2	4± 2	21±5	21± 5
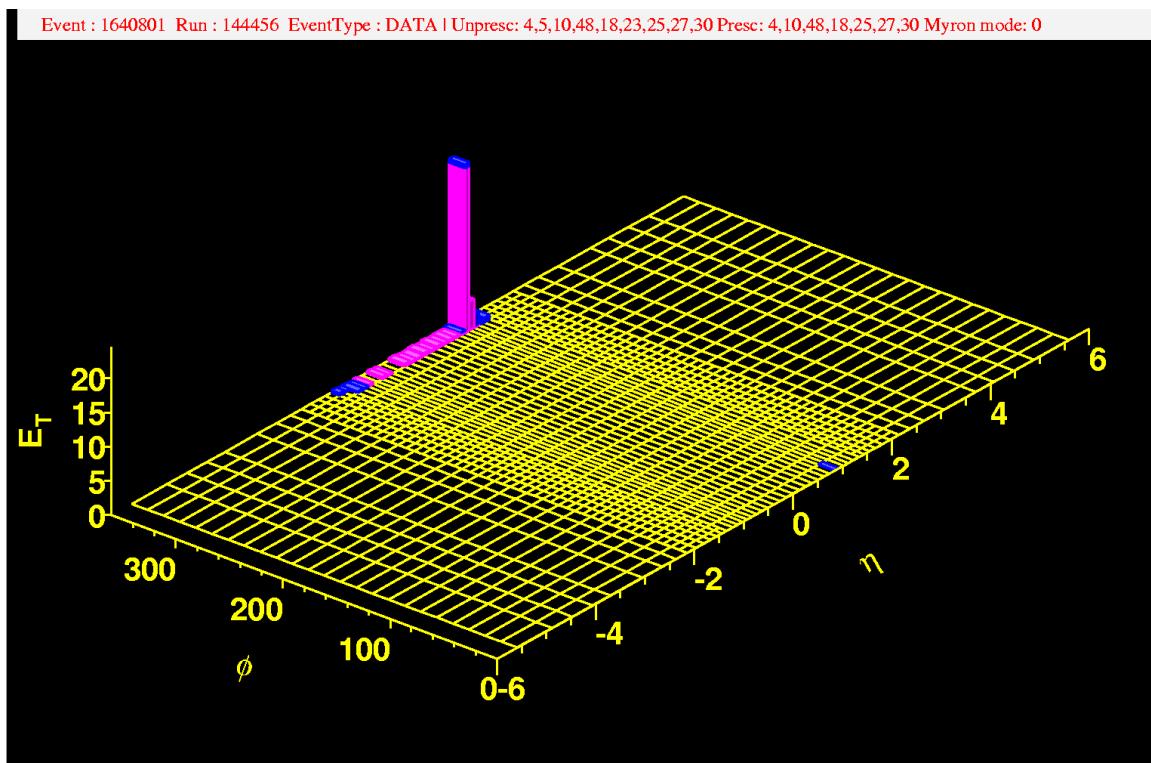
Fig. 1. CDF event display showing the energy deposited in the calorimeters as a function of location in the calorimeter (η, ϕ), where $\eta = -\log(\tan\frac{\theta}{2})$ and ϕ is the azimuthal angle. Protons enter from the $-\eta$ side.
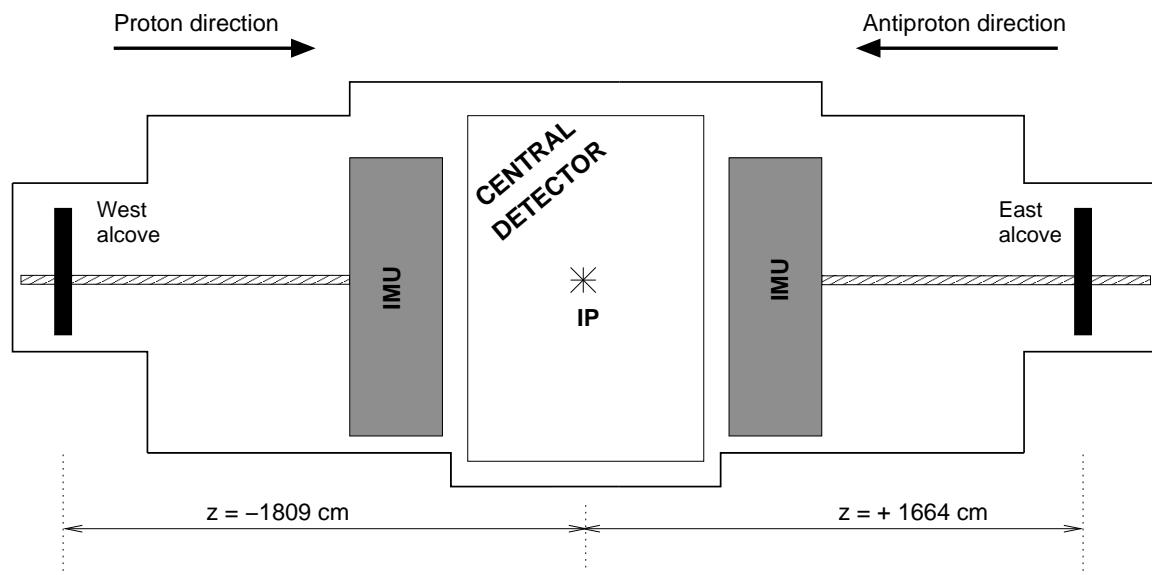
Fig. 2. Elevation of the CDF collision hall showing the positions of the halo monitors (not to scale). The proton monitor is located at $z = -1809$ cm and the antiproton monitor is at $z = +1664$ cm.
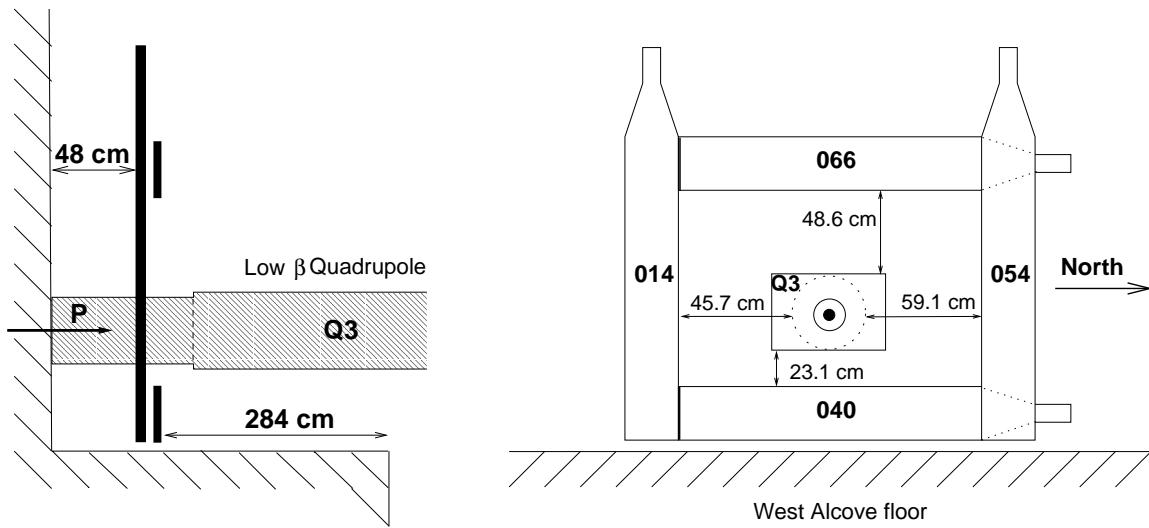
Fig. 3. Configuration of the proton halo counters around the low β quadrupole in the west alcove. The left figure is the side view and the right figure shows the view with protons exiting out of the page.
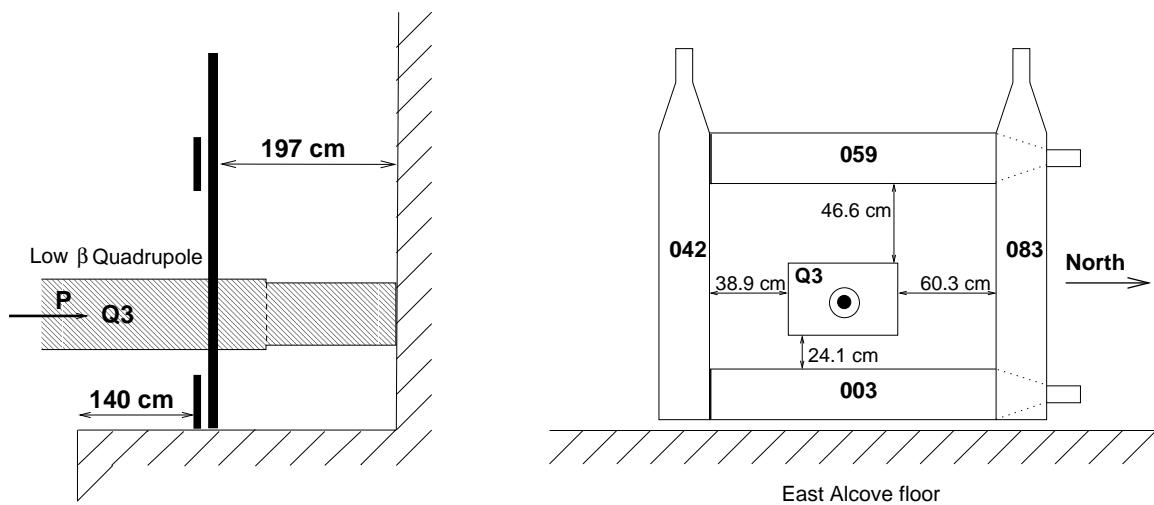
Fig. 4. Configuration of the antiproton halo counters around the low β quadrupole in the east alcove. The left figure is the side view and the right figure shows the view with protons exiting out of the page.

Scintillator

light guide

PMT/base

15 cm

150 cm

29 cm
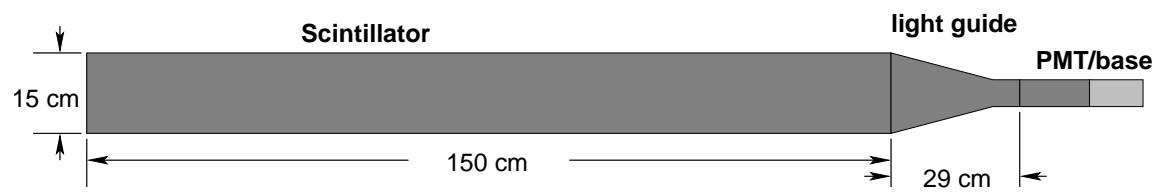
Fig. 5. Diagram of one scintillator counter used for the halo monitors.

CDF B0

CDF BC

CDF ABORT
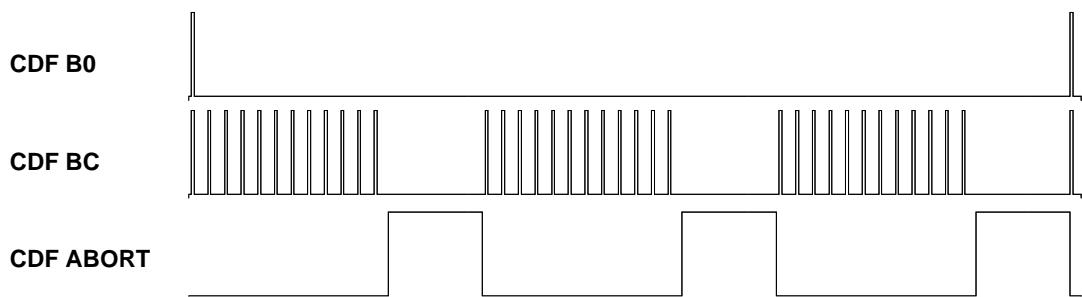
Fig. 6. Accelerator timing signals. The time between successive CDF_B0 events is one Tevatron revolution (20.7 μs).
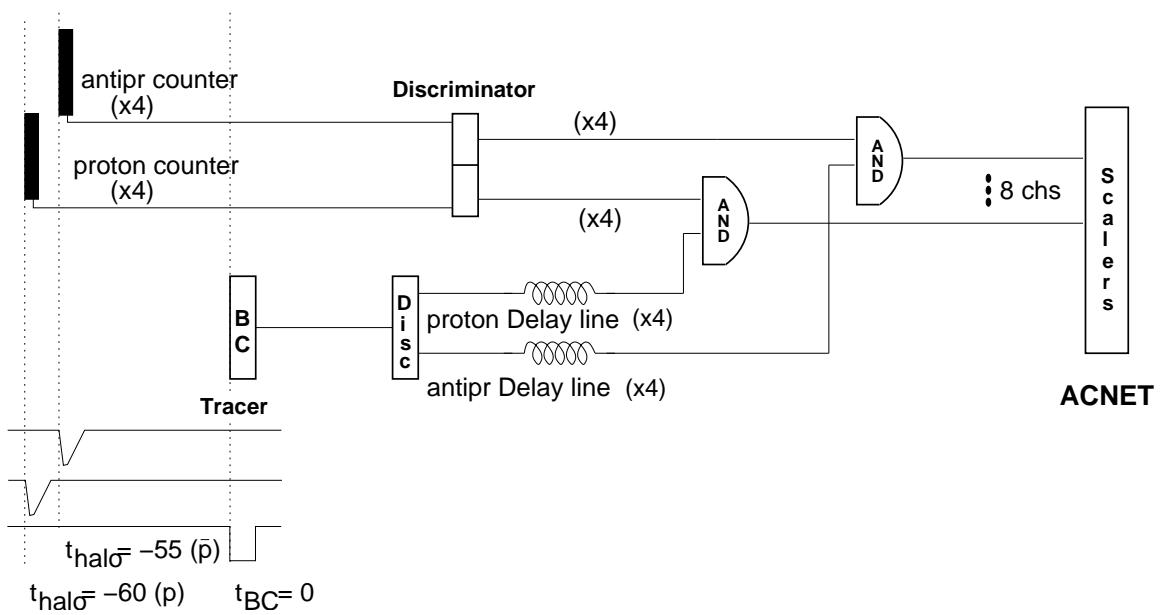
Fig. 7. Logic diagram for the beam halo monitors. The relative timing is also shown.
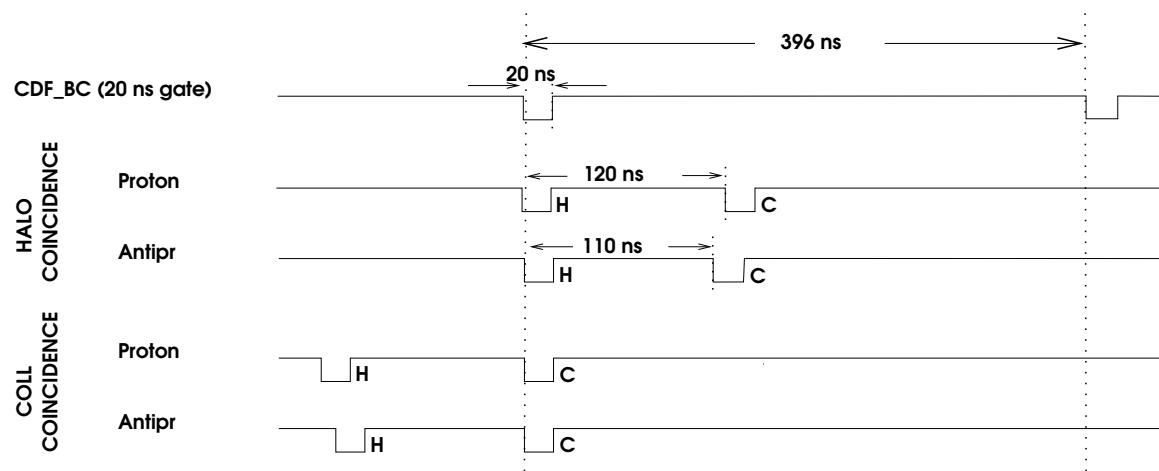
Fig. 8. Timing diagram for halo coincidences. It is possible to trigger for both halo (H) and collision debris (C) by application of appropriate delays.
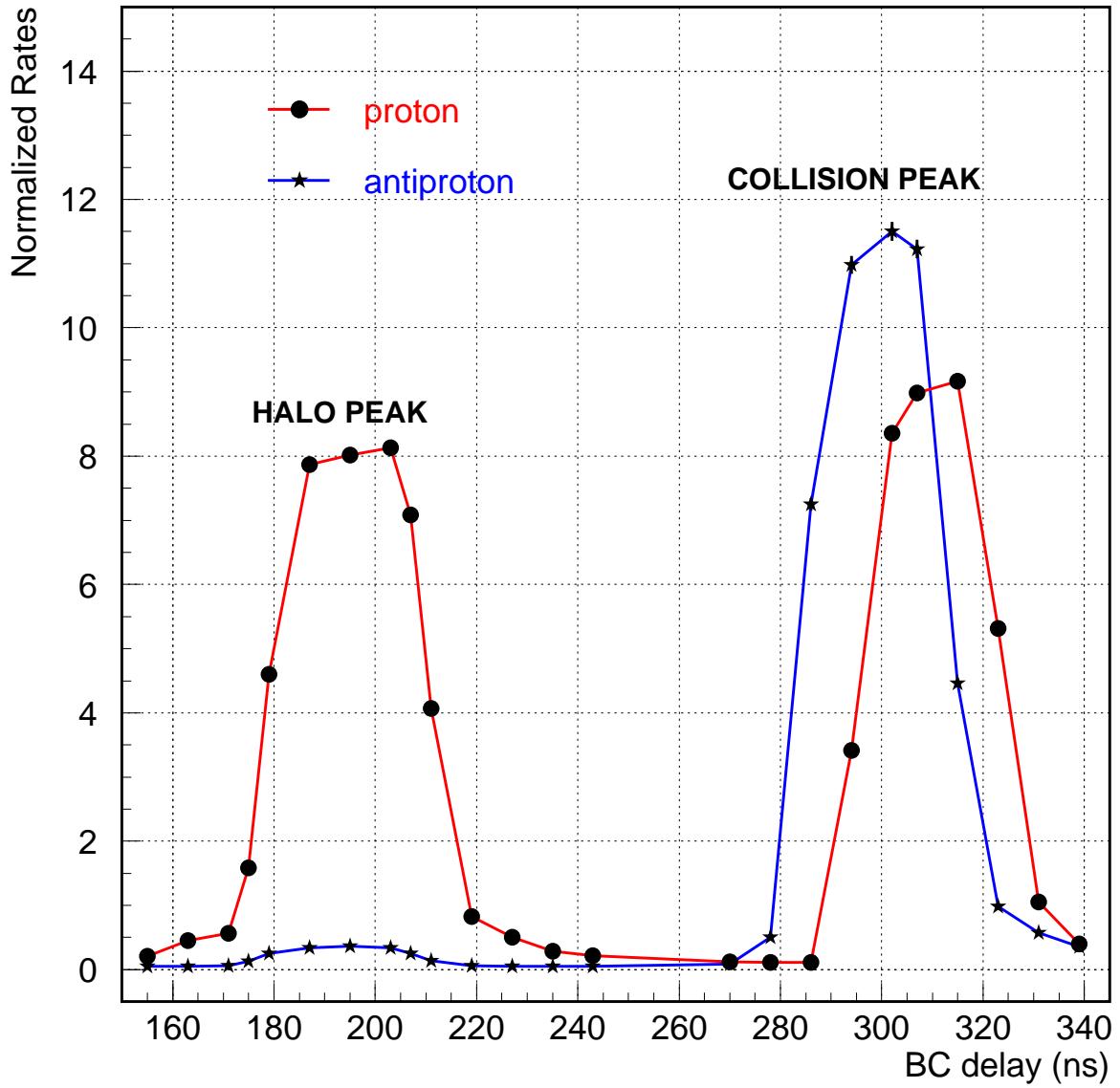
Fig. 9. Halo counter rates vs CDF_BC delay. The left peak is from the incoming beam halo; the right peak is from collisions. Statistical errors are also shown at each data point. The differing size of the halo peaks is due to the difference in the proton and antiproton beam currents.
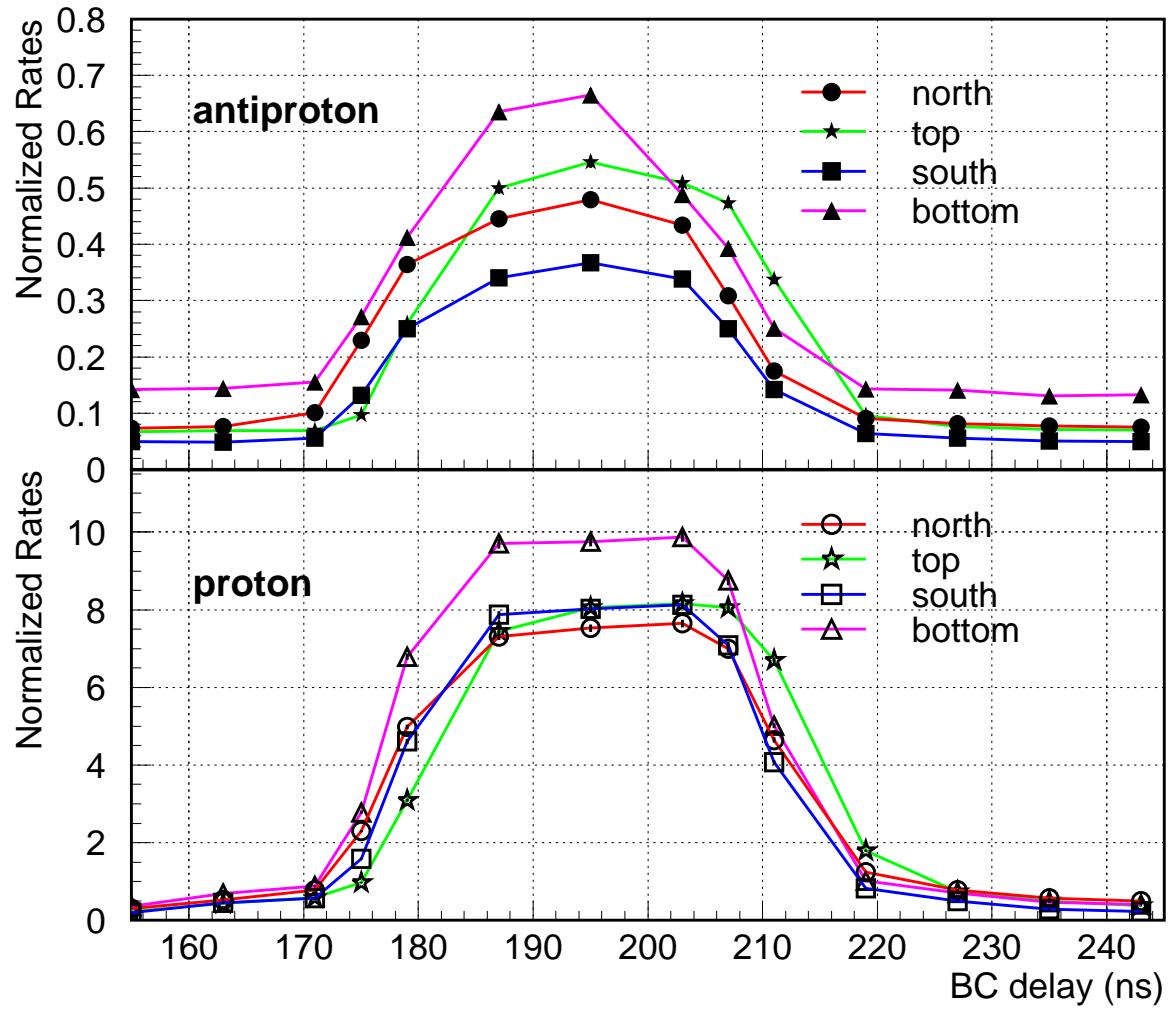
Fig. 10. The portion of the CDF_BC delay curve showing the halo coincidence plateaus.
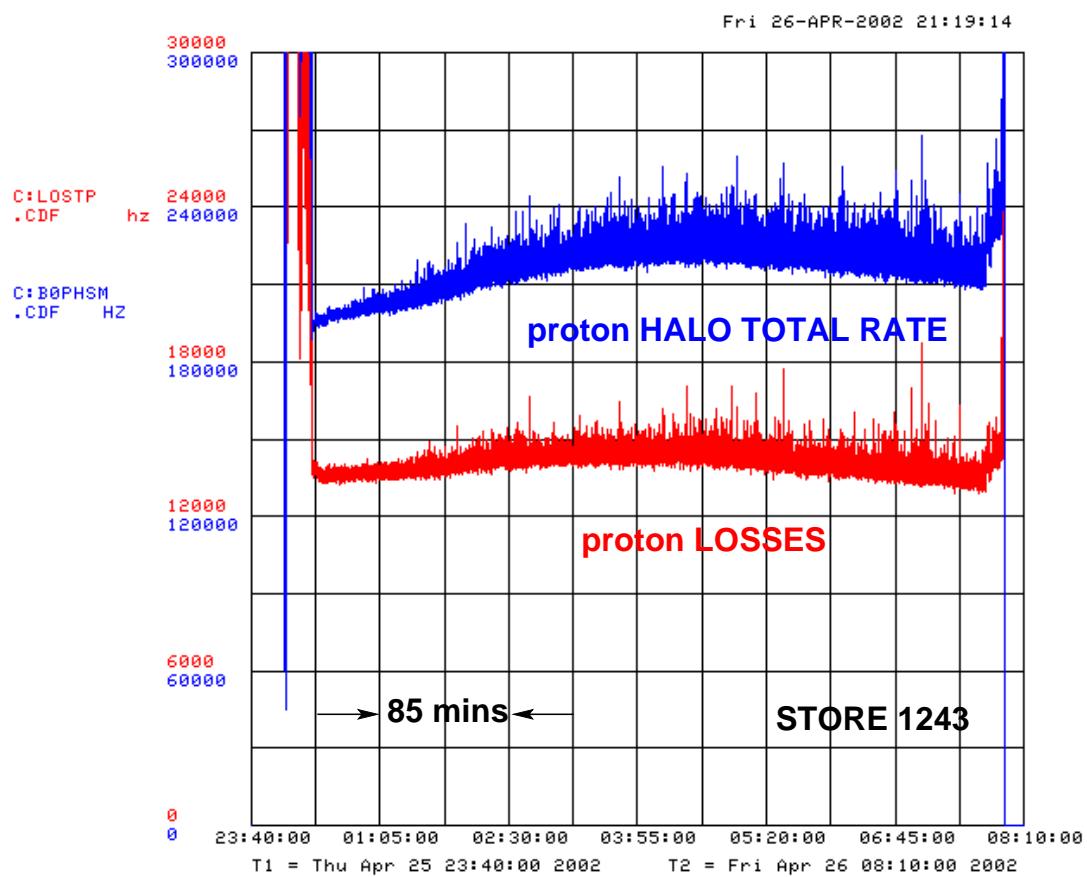
Fig. 11. Total proton halo rates (C:B0PHSM, bottom scale values) and proton losses (C:LOSTP, top scale values) vs time for store 1243.

21
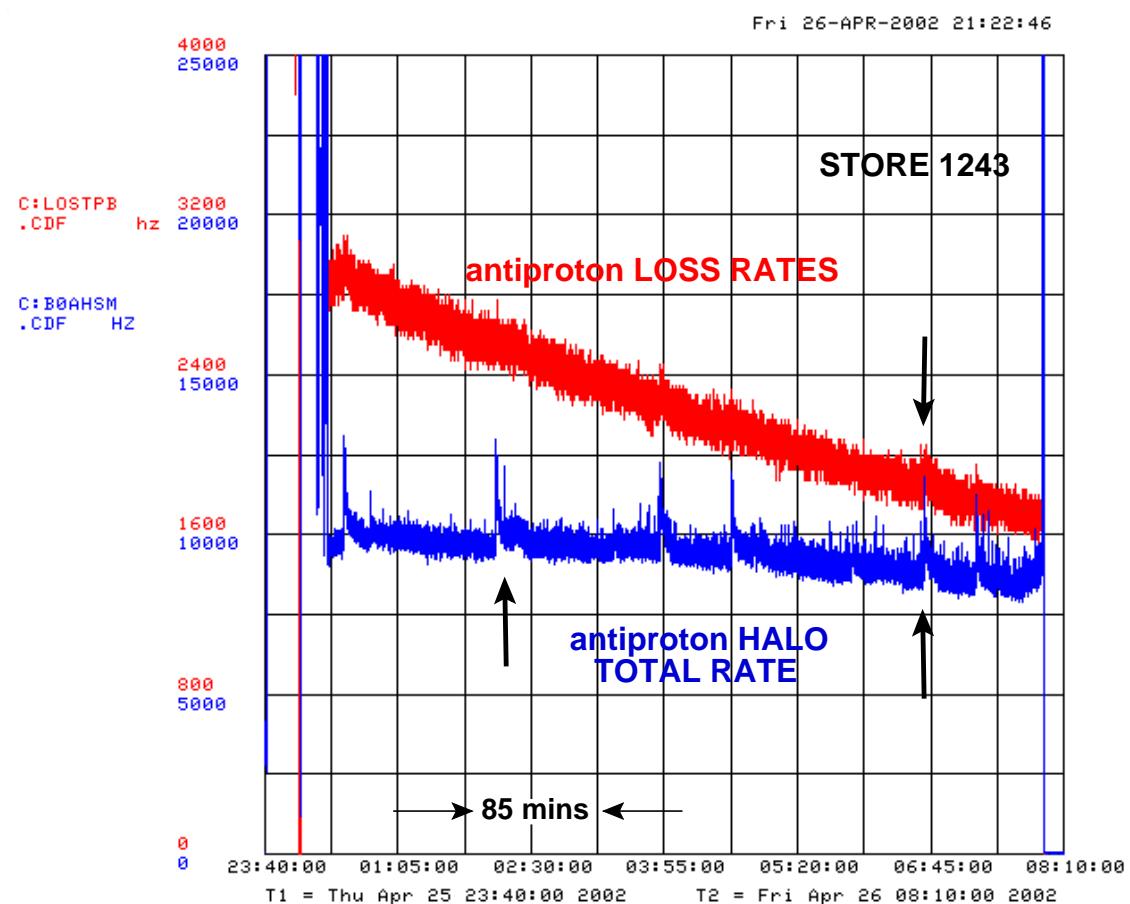
Fig. 12. Total antiproton halo rates (C:B0AHSM, bottom scale values) and loss rates (C:LOSTPB, top scale values) vs time for store 1243. Arrows indicate new features previously unnoticed.
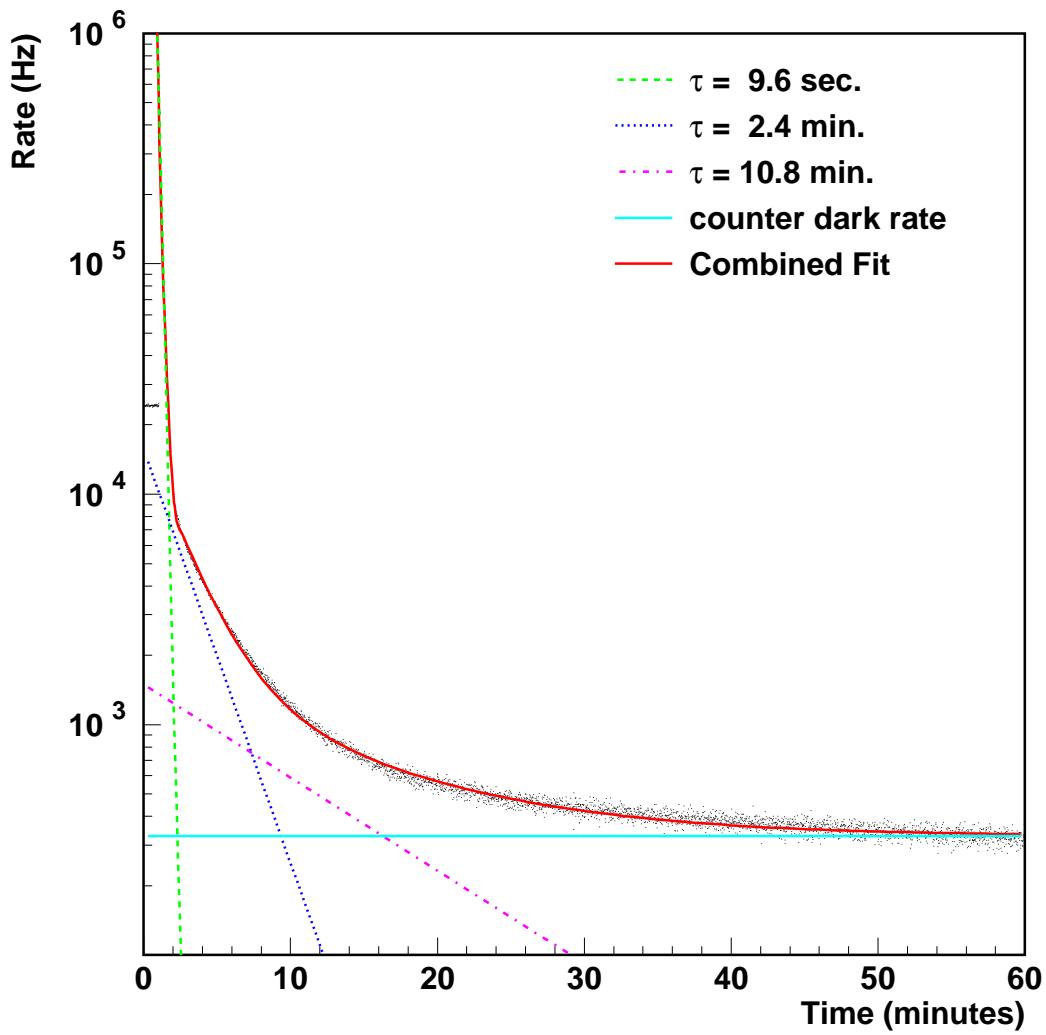
Fig. 13. Proton abort gap halo rate vs time after a Tevatron beam abort. The curve represent a fit to three exponentials plus a constant. The decay constants are consistent with the decays from three short lived potassium isotopes: ^{38}K, ^{46}K and ^{48}K.
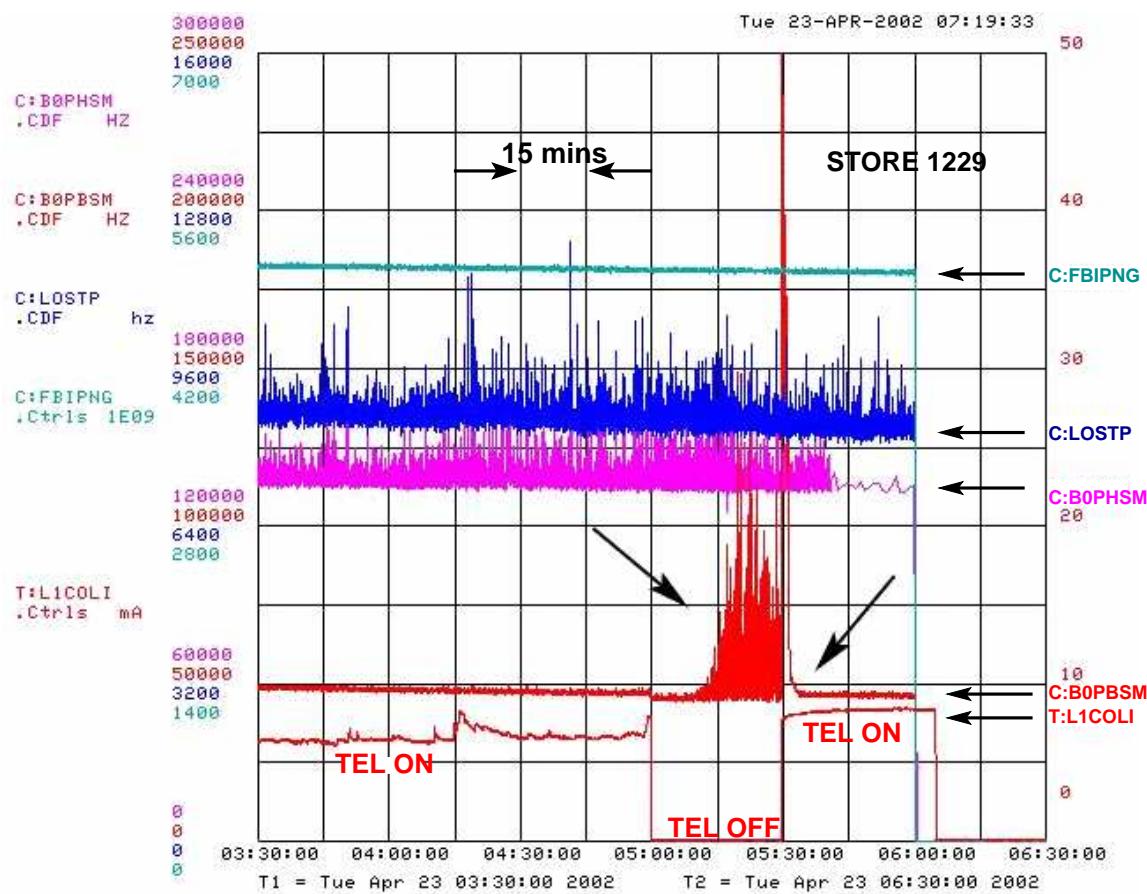
Fig. 14. Various ACNET variables vs time for a portion of store 1229. The large arrows indicate the sensitivity of proton abort gap halo monitor (C:B0PBSM) to Tevatron electron lens (T:L1COLI) being turned on. C:FBIPNG is the proton beam current in the Tevatron. The TEL was off for approximately half an hour.

24
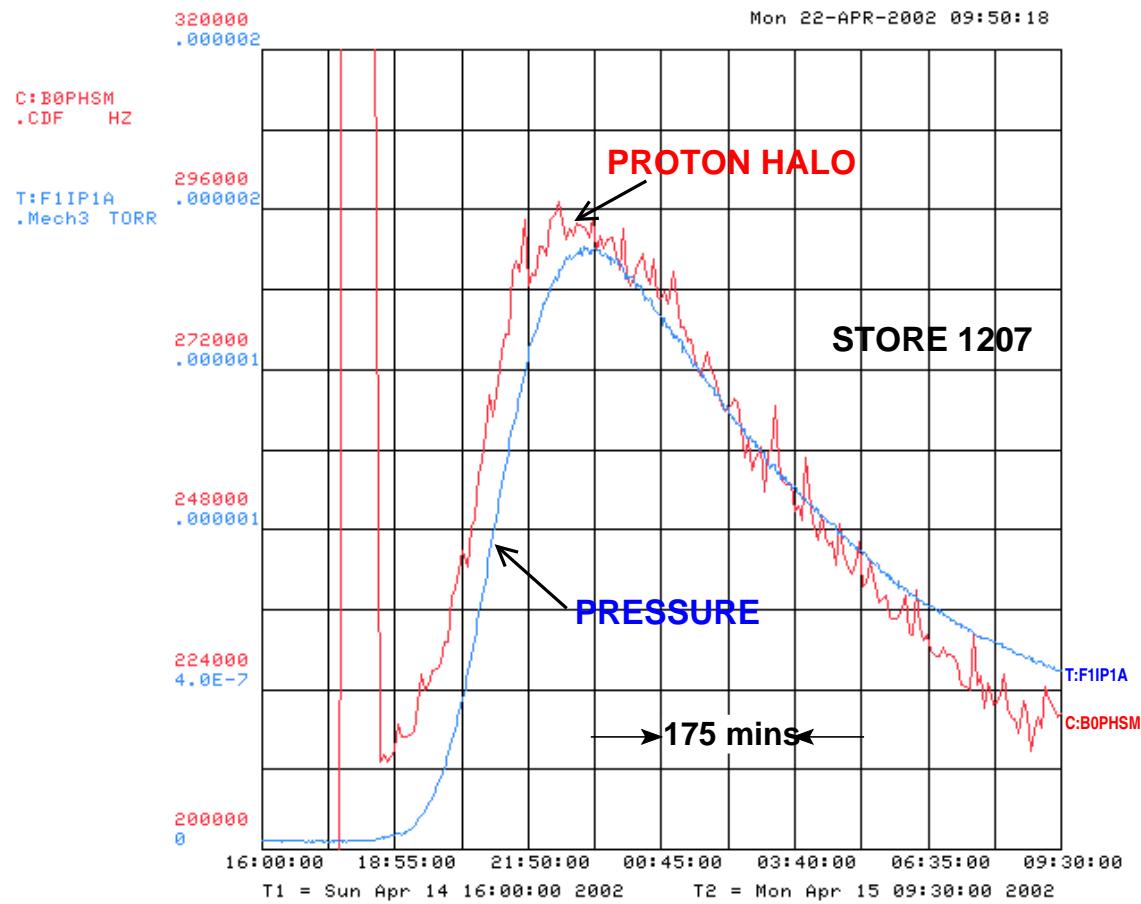
Fig. 15. Total proton halo rate (C:B0PHSM) and the vacuum measured in the Tevatron F11 sector (T:F1IPA) vs time for store 1207.
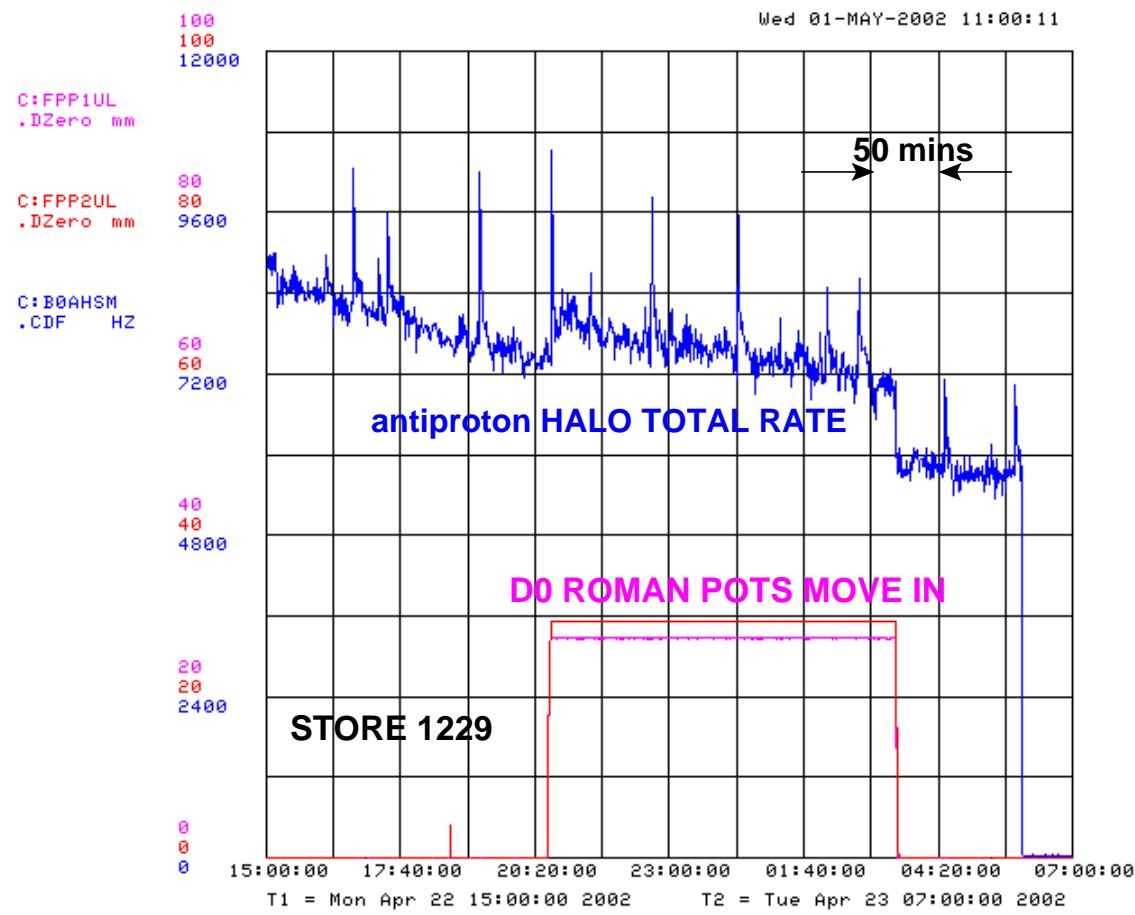
Fig. 16. Total antiproton halo rate (C:B0AHSM) and the DØ roman pot positions vs time during store 1229. The antiproton halo rate increases as the DØ roman pots are inserted.
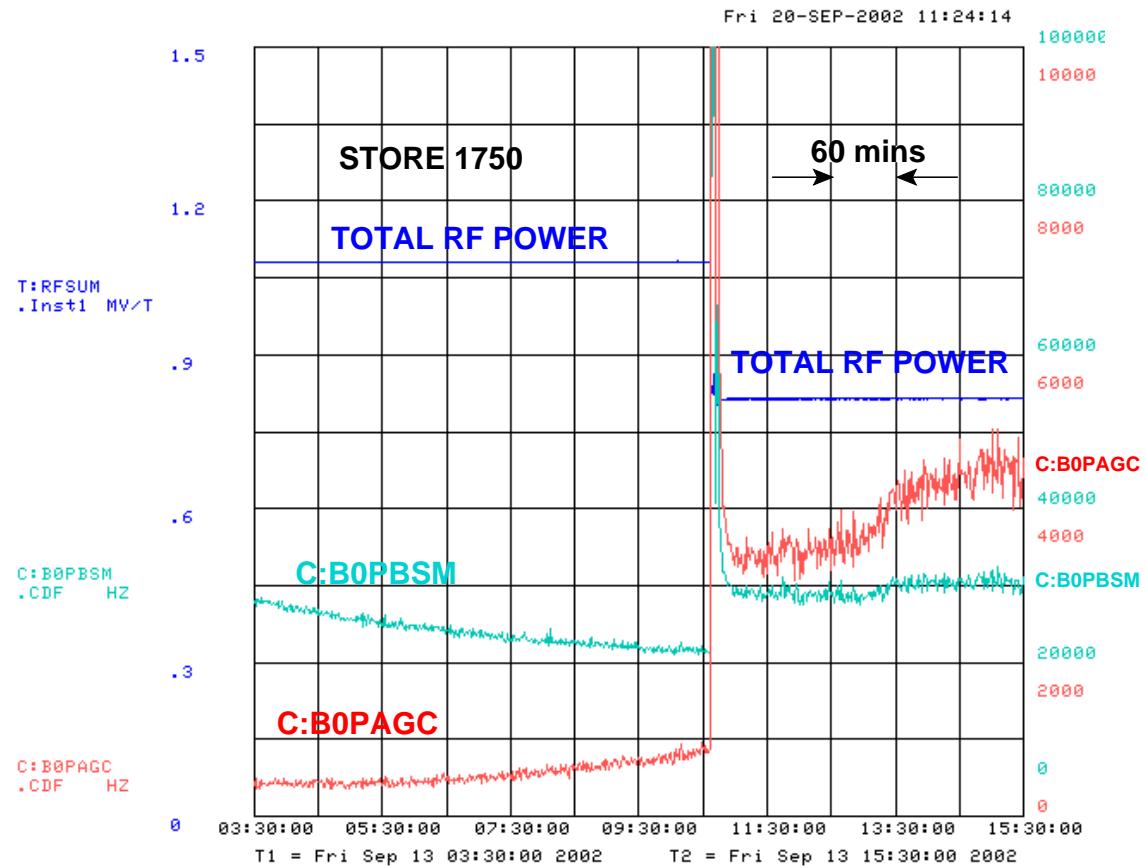
Fig. 17. Total proton abort gap halo (C:B0PBSM) and 2/4 majority coincidence (C:B0PAGC) rates vs time for a portion of Tevatron store 1750. The power was lost for an RF cavity around 10:20AM on September 13th, 2002.